Supplemental Figure Legends and Methods

Supporting Information Corrected June 12, 2014

Figure S1: α-Cat protein expression across cell lines

A. Epifluorescence image (Zeiss Axioplan) of methanol fixed Madin Darby Canine Kidney (MDCK) cells stably knocked-down for endogenous dog α-cat and restored with GFP-mouse α-cat. Panels indicate intrinsic GFP fluorescence, β-cat immuno- and Hoechst DNA- staining. Scale bar = 10μm. Note that GFP-α-cat is largely nuclear excluded in these cells, as previously shown (Arrows) (1). **B.** Western blot of α-cat protein levels in Wnt-pathway activated cancer cell lines (SW480 and DLD1) versus non-transformed MDCK using Enhanced Chemiluminescence (ECL)/film exposure method. Note that total α-cat protein levels are similar between transformed (SW480/DLD1) and non-transformed (MDCK) cell lines. Band intensities were quantified using Image J software and plotted in **C.**

Fig. S1: α-cat expression levels across cell lines

A.

B.

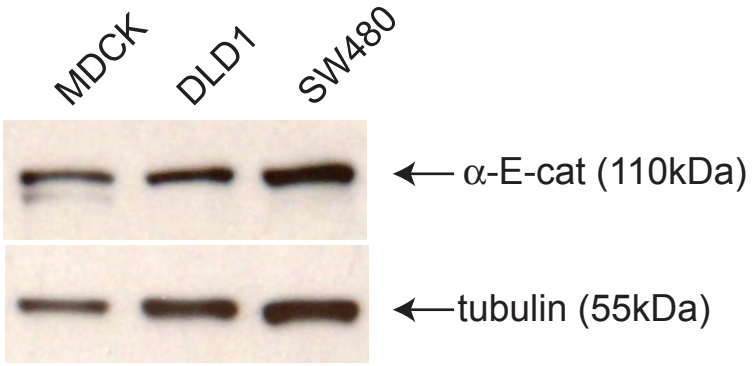

C.

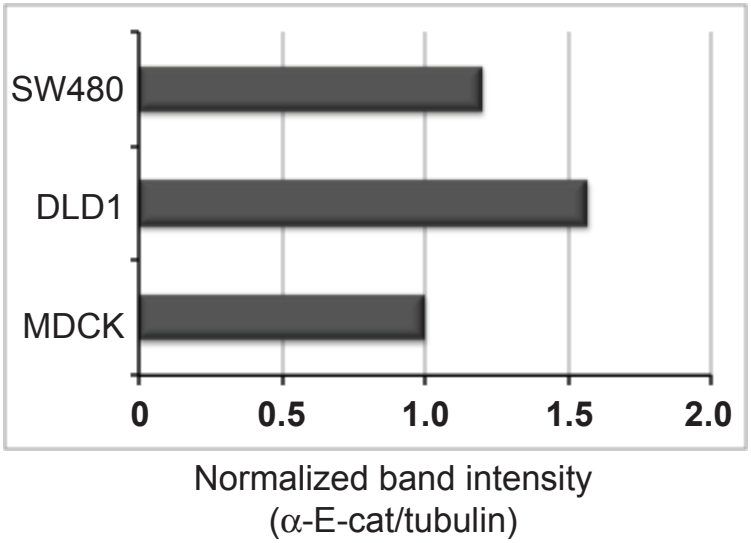

Figure S2: Characterization of nuclear α-cat localization

A. Epifluorescence images of methanol fixed SW480 cells stained with Hoechst (DNA) and monospecific antibodies to α-cat (3C1 and 3H4 (2)) and β-cat. **B.** Confocal image of methanol fixed SW480 cells stained with α-cat monoclonal antibody 5B11(2) and β-cat. **C.** Similar to Fig. 1, this is an epifluorescence image of methanol fixed SW480 cells transiently transfected with control and β-cat siRNAs (Dharmacon Smartpool, see Methods) and stained with antibodies to α-cat (monoclonal antibody, 6A1(2)) and β-cat (Cell Signaling). Asterisk and dotted lines denote region of β-cat knock-down, where α-cat is redistributed to the cytoplasm. **D.** LI-COR western blot image of SW480 and DLD1 cells separated into cytoplasmic (Cyto), membrane (Mem) and nuclear fractions (as described in Methods), separated by SDS-PAGE, blotted with the antibodies indicated. Note that increasing the concentration of sucrose in the washes depletes E-cadherin, but not α-cat nor β-cat.

Fig. S2: Characterization of nuclear α-cat immunolocalization

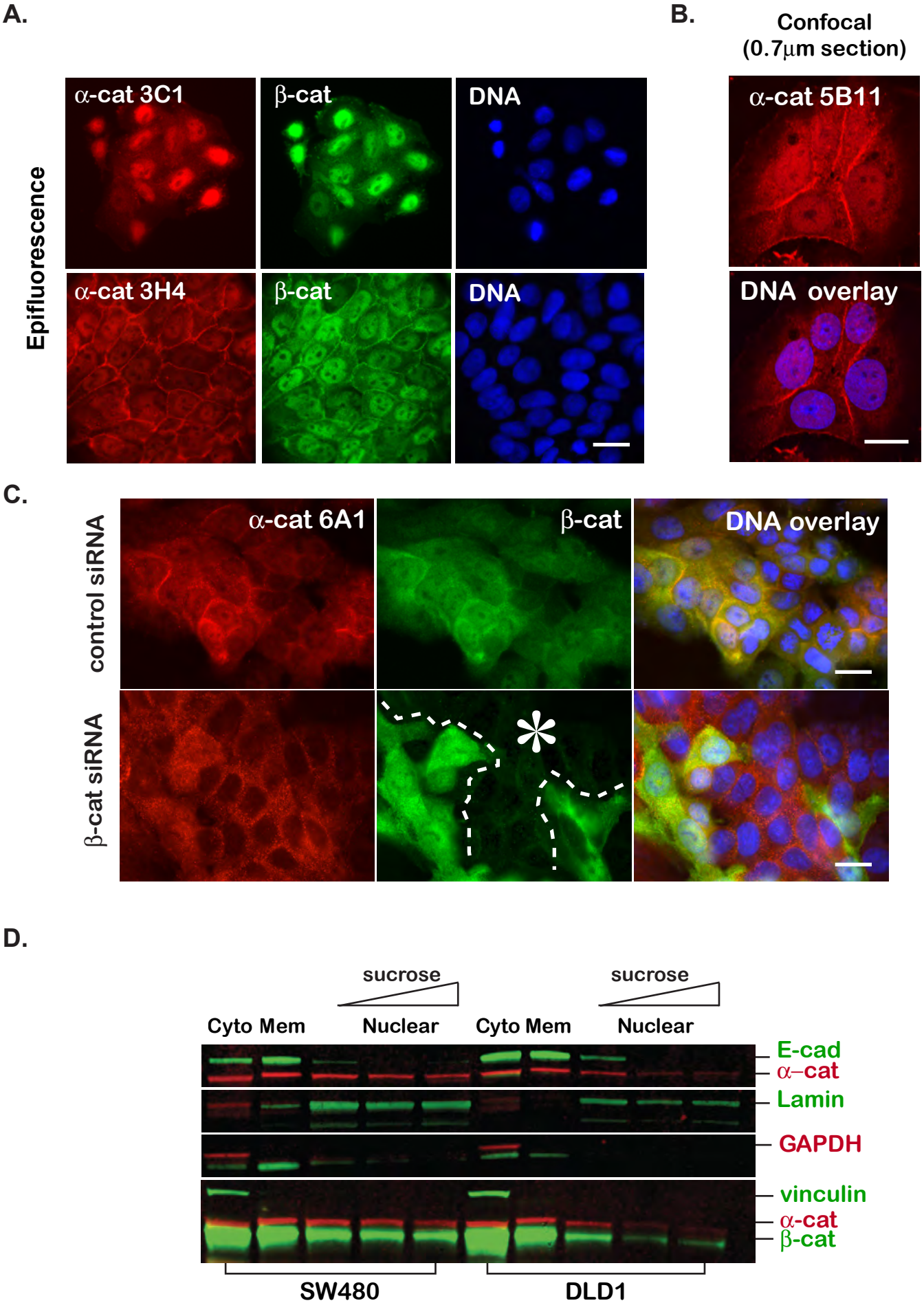

Figure S3: Wnt3a and the β-cat binding domain promote nuclear accumulation of α-cat

A. Immunoblot (IB) of -/+Wnt3a stimulated (36 hours) HEK293T cells separated into cytosolic and nuclear fractions and incubated with tubulin and acetylated histone H3 antibodies to mark cytosolic and nuclear fractions. Note the Wnt3a-dependent shift in α-cat from cytosolic to nuclear-enriched fraction. **B**. Immunoblots of HEK293T cells transfected with either mycWT-α-cat or mycΔβBD-α-cat and separated into cytosolic and nuclear fractions and probed with the antibodies indicated. Note that α-cat lacking the β-cat binding domain (mycΔβBD-α-cat) fails to associate with a nuclear fraction to the same extent as mycWT-α-cat. **C.** Epifluorescence images of MDA-MB-231 human breast cancer cells treated with Wnt3a or control conditioned media (CM) for 16 hours before fixation and processing for immunofluorescence with the antibodies shown. **D.** Western blot (WB) from cells treated as in C. Immunoblotting antibodies shown.

Fig. S3: Wnt3a and the β-cat-binding domain promote nuclear accumulation of α-cat

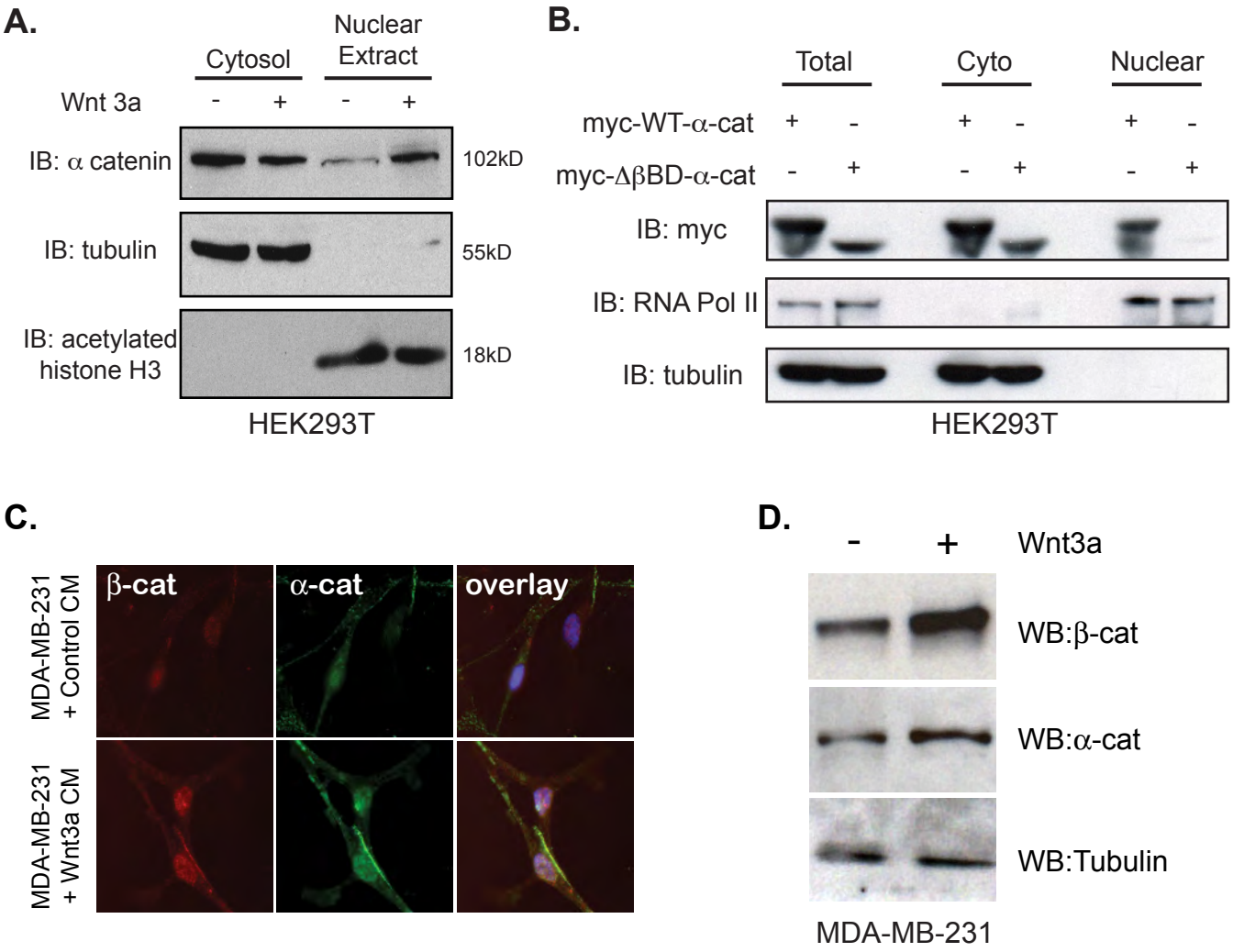

Figure S4: α-Cat inhibits Wnt signaling

A. β-cat/TCF-reporter assay (TOPflash) of HEK293T cells transfected with Wnt3a -/+ increasing doses of α-cat. TOPflash data is normalized to Pol III Renilla and a reporter lacking TCF-consensus sites (FOPflash). **B**. qPCR of *C-MYC* expression in HEK293T cells transfected with Wnt -/+ α-cat. *C-MYC* was normalized to 18S and fold induction calculated with the ΔΔCt method. Error bars reflect standard deviations from 4 (A) and 3 (B) independent experiments.

Fig. S4: α-cat inhibits Wnt3a signaling (over-expression)

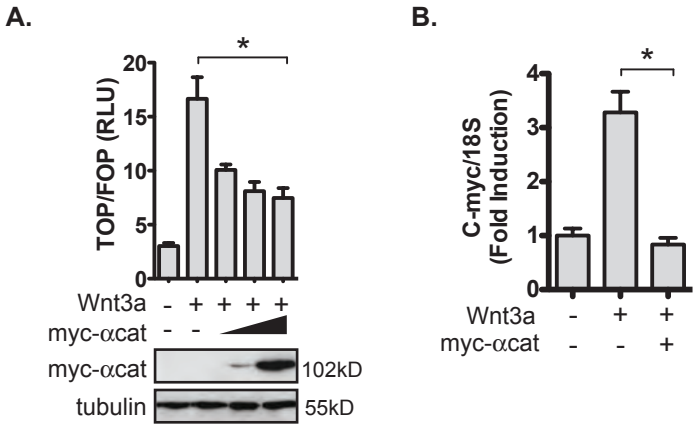

Figure S5: α-Cat interacts with β-cat and TCF

A. Immunoblot from affinity precipitation of 6xHistidine(His)-Tobacco Etch Virus (TEV protease site)-tagged α-cat expressed in α-cat null R2/7 DLD1 cells; affinity precipitation from nuclear-enriched fraction. **B.** Immunoblot of TCF4 immunoprecipitation from SW480 cell fractions. Respective western blotting (WB) antibodies are shown.

Fig. S5: α-cat interacts with β-cat and TCF4

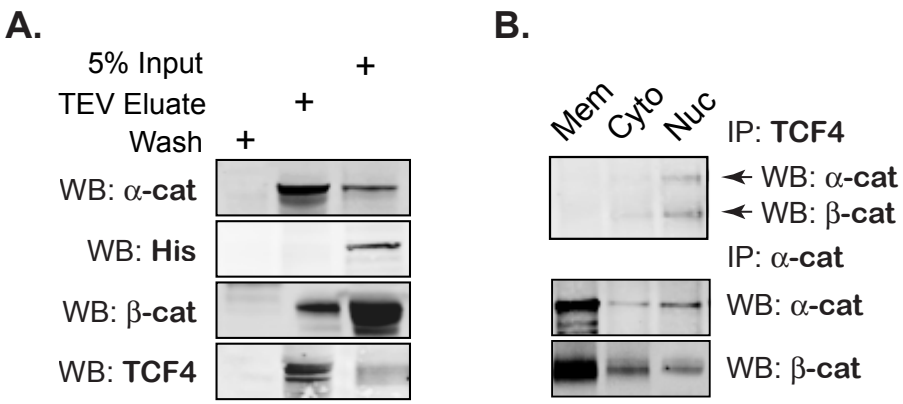

Figure S6: Inhibition by α-cat requires binding to β-cat

A. Diagram showing dimerization mutants of α-cat and β-cat. Deletion of amino acids 1-82 from α-cat generates a form lacking the β-cat-binding domain (mycΔβBD-α-cat). Deletion of amino acids 118-148 from β-cat generates a form lacking the α-cat binding domain (ΔαBD-β-cat-flag). **B**. HEK293T cells transfected with either the mycWTα-cat or mycΔβBD-α-cat were immunoprecipitated using a myc antibody and blotted with antibodies to myc, β-cat, and GAPDH (loading control). **C**. HEK293T cells transfected with either the WT β-cat-flag or ΔαBD-β-cat-flag were immunoprecipitated using the flag epitope and blotted with antibodies to flag, α-cat, and GAPDH. **D**. Transfection of HEK293T cells with mycWT-α-cat inhibits Wnt3a signaling using the β-cat/TCF-OPtimal reporter assay (TOPflash), while the mycΔβBD-α-cat has no effect. **E**. Transfection of HEK293T with mycWT α-cat inhibits WT-β-cat-flag but not ΔαBD-β-cat-flag in the TOPflash assay. TOPflash data is normalized to Pol III Renilla and a reporter lacking TCF-consensus sites (FOPflash). Error bars represent SEM of triplicate transfections (* $p < 0.05$ by t-test).

Fig. S6: Inhibition by α-catenin requires binding to β-catenin

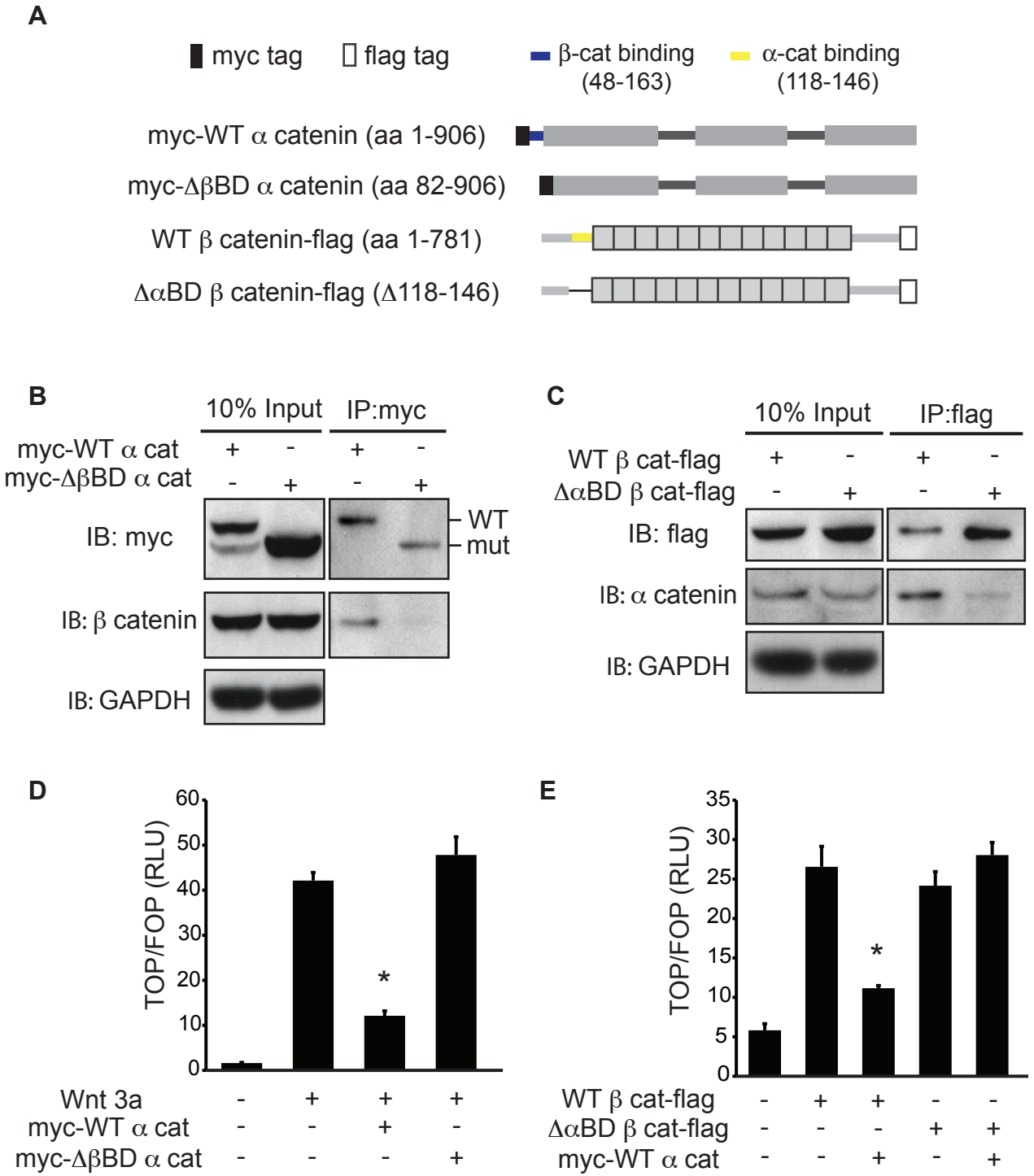

Figure S7: Inhibition by α-cat requires dimerization and actin-binding domains

A. Diagram showing C-terminal truncation mutants of mycWT α-cat. **B**. Expression of α-cat C-terminal mutants in HEK293T TOPflash reporter assay. **C&D**. Western blot and diagram of α-cat N-terminal fragments encoding β-cat and α-cat dimerization regions. **E.** HEK293T cells transfected with myc-α-cat 1-163 and/or myc-α-cat 82-279 show enhanced Wnt3a-specific activation of the TOPflash reporter. Expression of either N-terminal fragment alone slightly enhances Wnt signaling but co-expression of both fragments additively activates Wnt signaling. **F.** Expression of either myc-α-cat 1-163 or myc-α-cat 82-279 relieves inhibition of the TOPflash reporter plasmid by mycWT-α-cat. Error bars represent standard deviation of triplicate samples. Asterisk denotes $p<0.05$ by t-test of condition compared to Wnt3a treatment.

Fig. S7: Inhibition by α-catenin requires dimerization and actin binding-domains

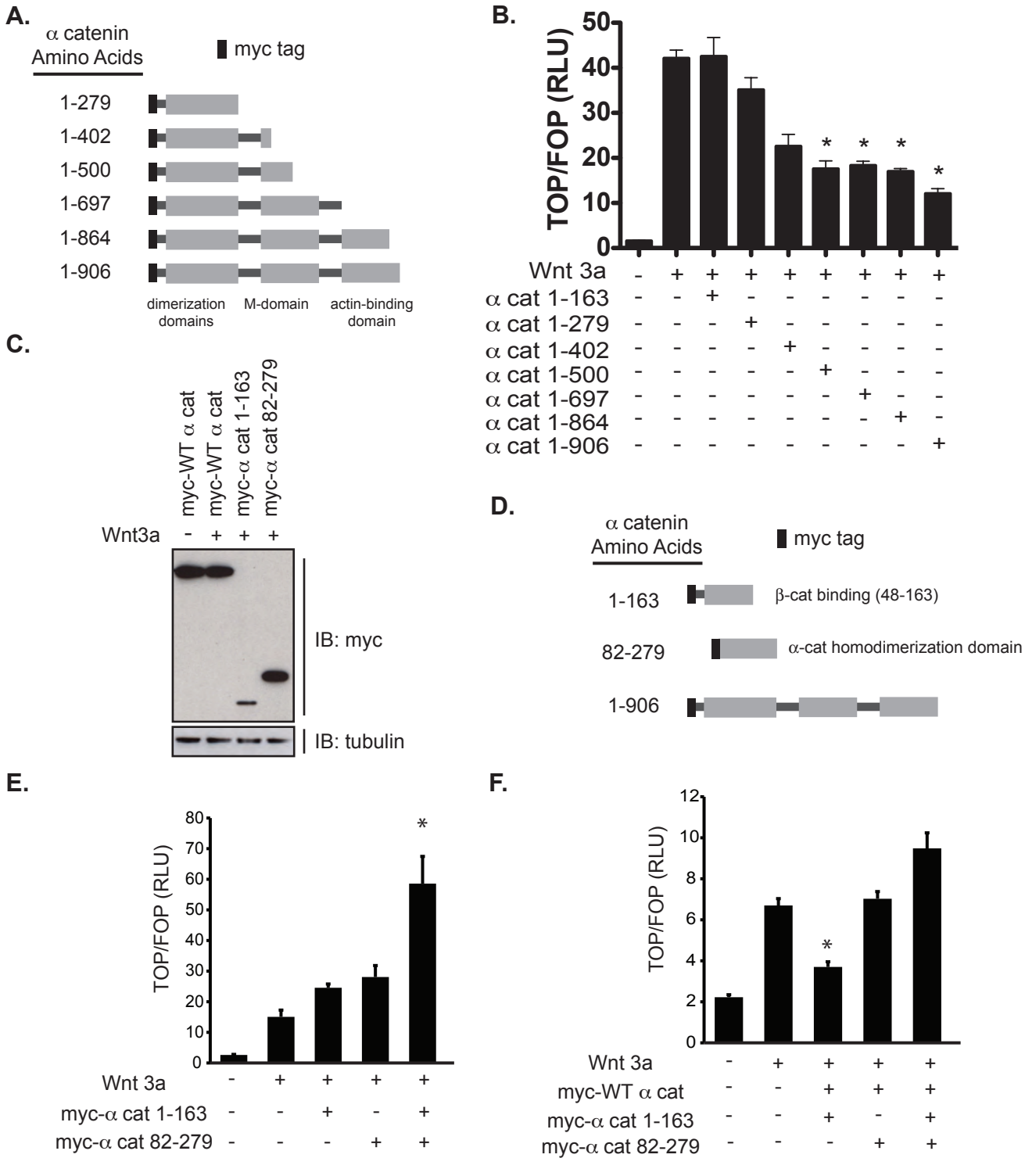

Figure S8: α-Cat deletion mutants are detected in an enriched nuclear fraction. HEK293T cells transfected with the α-cat C-terminal mutants were fractionated into cytosolic and nuclear extracts. Fractions were analyzed by SDS-PAGE and blotted for myc (α-cat), tubulin (cytosolic), and lamin A/C (nuclear).

Fig. S8: α-cat deletion mutants are detected in a enriched nuclear fraction

A.

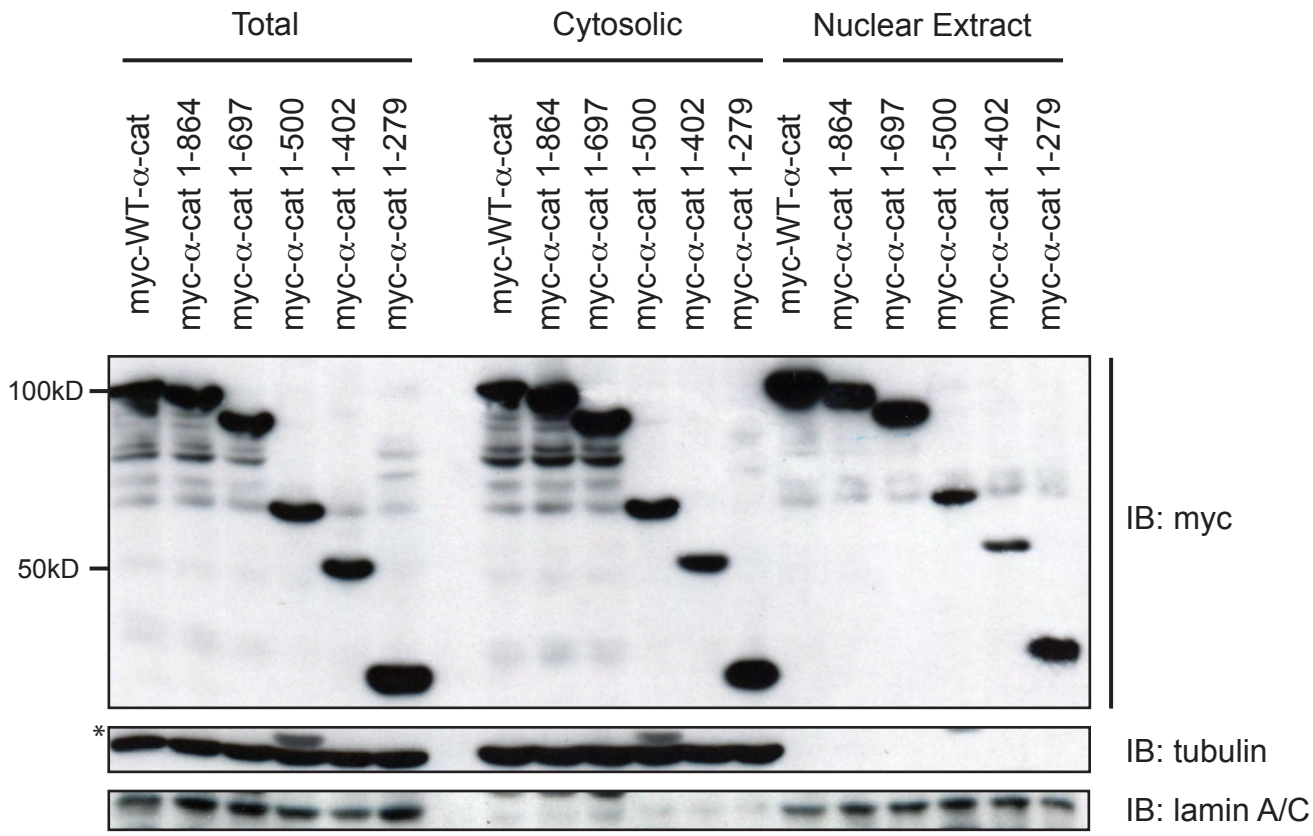

Figure S9. α-Cat actin binding domain is required and sufficient for nuclear F-actin staining

A-H. COS7 cells mock transfected (**A**) or transfected with mycNLS-α-cat 1-163 (**B**), mycNLS-α-cat 1-402 (**C**), mycNLS-α-cat 1-500 (**D**), mycNLS-α-cat 1-697 (**E**), mycNLS-WT-α-cat (1-906) (**F**), mycNLS-α-cat 82-906 (lacking the β-cat-binding domain, **G**), mycNLS-α-cat 697-906 (contains the minimal F-actin-binding domain, **H**) were processed for immunofluorescence using antibodies to myc and phalloidin. Nuclei are stained with Hoechst and merged images are shown. Scale bar = 20 μm.

Fig. S9: α-cat actin-binding domain is required and sufficient for nuclear F-actin staining

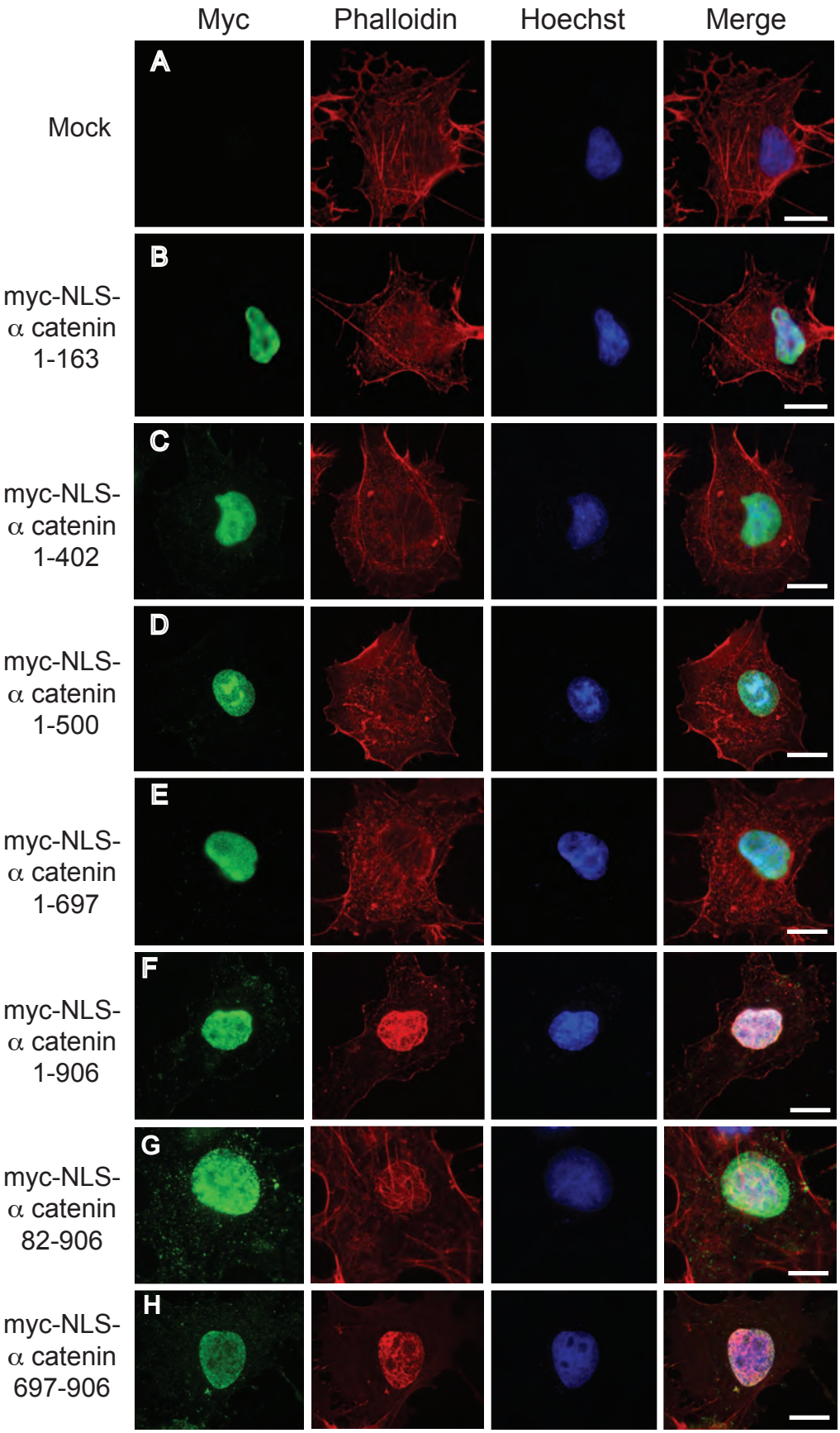

Figure S10: Characterization of NLS-α-cat C-terminal truncation mutants

A. Diagram showing mycNLS-α-cat C-terminal truncation mutants used in Fig. S9.

B&C. COS7 cells transfected with mycNLS-α-cat mutants described above were fractionated and analyzed by SDS-PAGE/immunoblotting with the antibodies indicated. Asterisk indicates location of mycNLS-α-cat 1-500 fragment on tubulin blot.

Fig. S10: Characterization of NLS-α-catenin C-terminal mutants

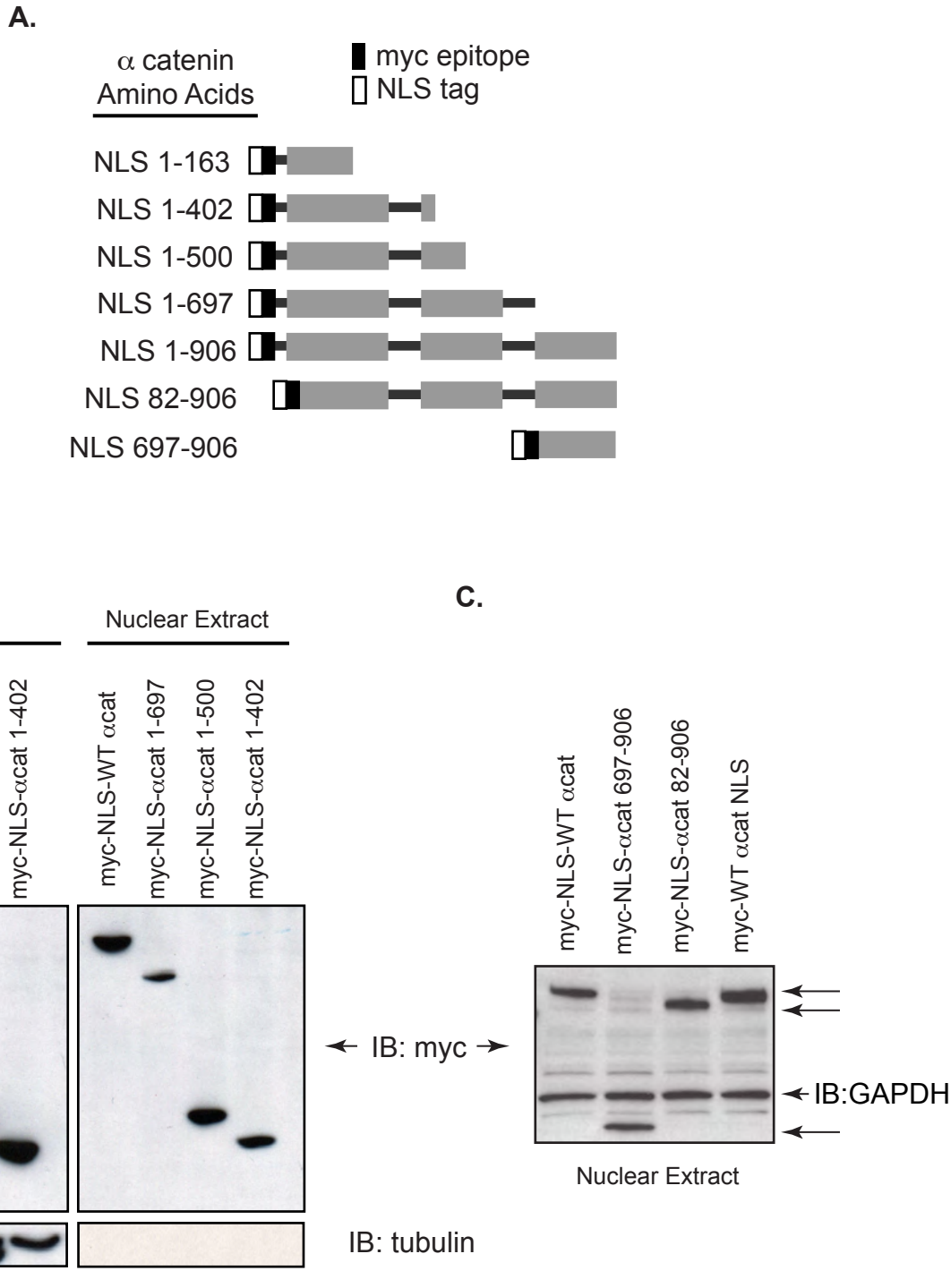

Figure S11: NLS-α-cat does not affect nuclear actin levels

A. COS7 cells transfected with GFP, mycWT-α-cat, or mycNLS-WT-α-cat were fractionated and analyzed by SDS-PAGE/immunoblotting for myc, actin, tubulin, and RNA polymerase II. **B**. COS7 cells transfected with EYFP-NLS-WT-actin (green) were stained with phalloidin to mark polymeric actin (red) and Hoechst to label DNA (blue). Note that increasing the amount of nuclear actin is not sufficient to induce formation of F-actin filaments. Scale bar = 20 μm.

Fig. S11: α-catenin does not affect nuclear actin levels

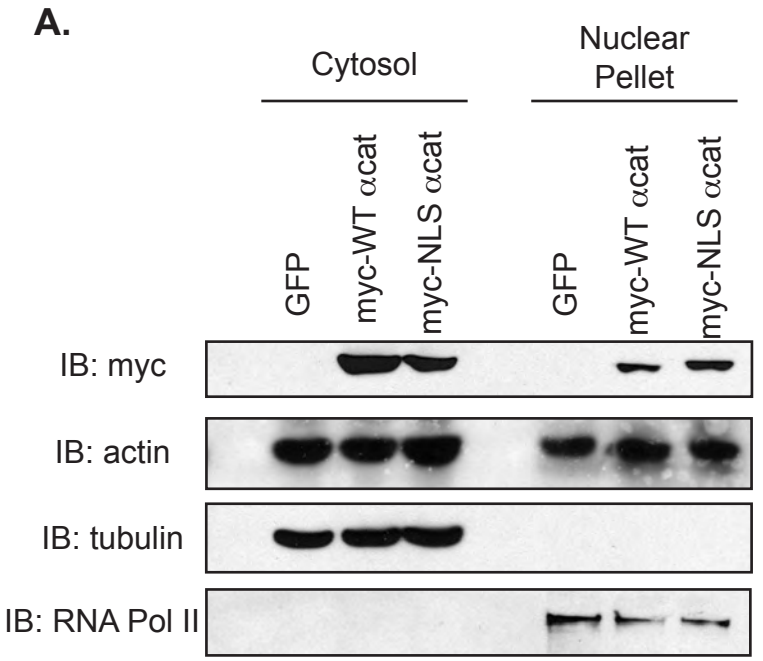

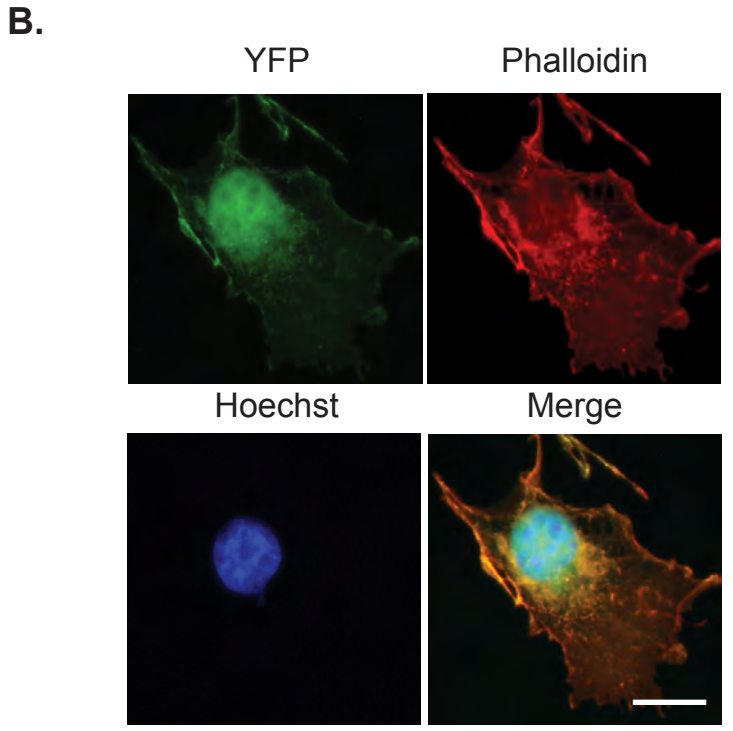

Figure S12: α-Cat impacts nuclear actin properties

A. Image of FRAP experiment for control silenced SW480 cells transfected with NLS-actin-YFP shown in Fig. 3C and described in Methods. **B.** Nuclear actin sedimentation assay. Nuclear extracts purified from SW480 control hairpin and α-cat shRNA expressing cells were centrifuged at 100,000g for 60 minutes, and supernatant and pellet fraction were fractionated by SDS-PAGE and immunoblotted with an antibody to actin. Blot represents single experiment. Graph represents average of 6 independent nuclear extract isolations from different α-cat shRNA hairpin expressing cell lines. Note that nuclei from α-cat KD cells show a reduced fraction of nuclear actin that can be pelleted relative to total nuclear actin. **C.** Representative image of data shown in Fig. 3D, where we sought to address whether α-cat could impact the capacity of a pathogenic mutant form of actin--known to cause Intranuclear Rod Myopathy (IRM)-- to form nuclear actin filaments. IRM is a dominant, skeletal muscle disease caused by mutations in actin (e.g., V163M α-actin) associated with nuclear actin filaments and muscle wasting (3). SW480 control hairpin and α-cat shRNA expressing cells are transfected with NLS-β-actin and V163M α-actin, both of which have the capacity to form nuclear actin filaments (arrows). SW480 cells lacking α-cat show a reduced capacity to form nuclear actin filaments. Asterisks denote statistical significance by t-test.

Fig. S12: α-cat impacts nuclear actin properties

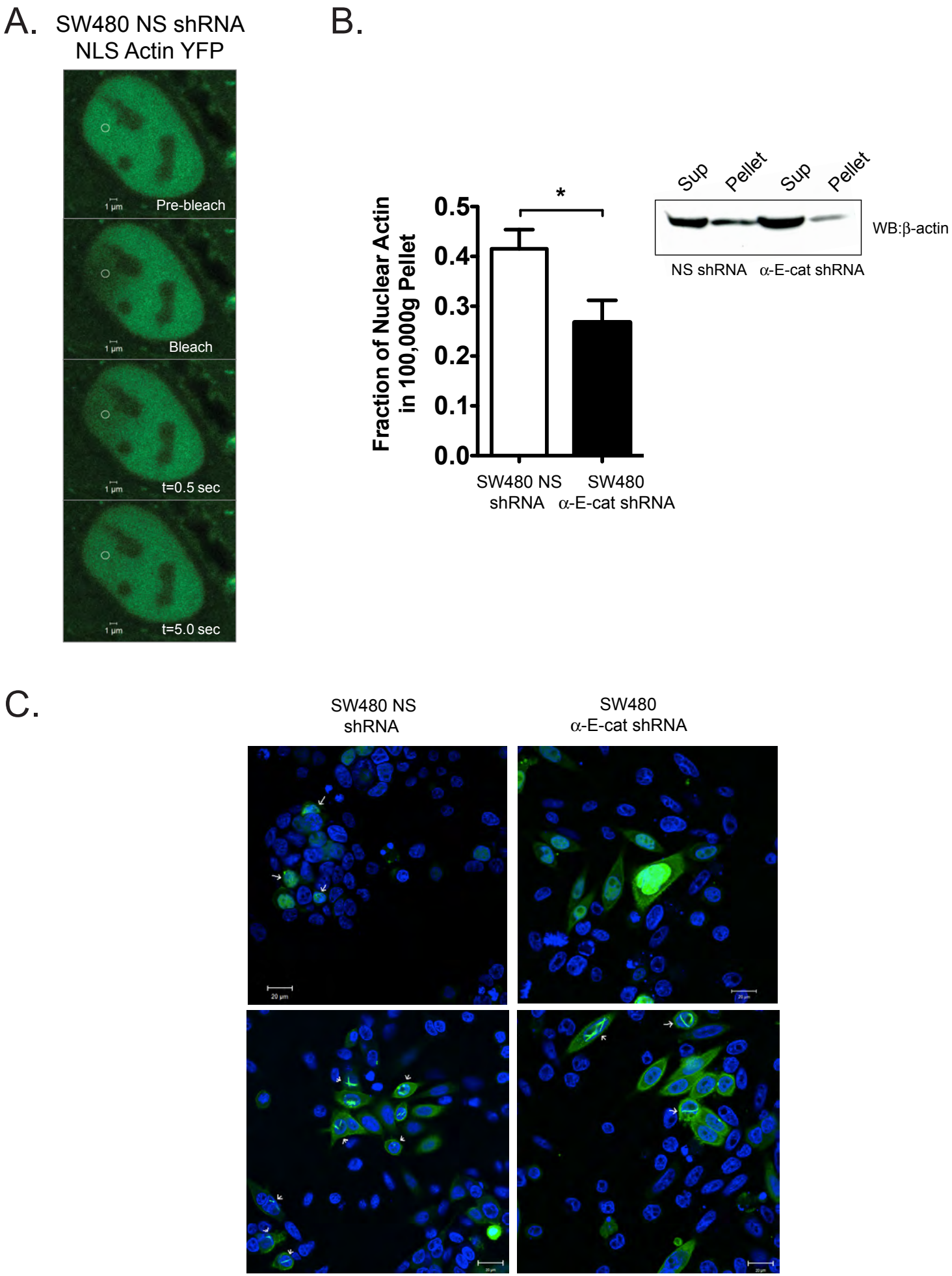

Figure S13: Immunofluorescence images of BrU incorporation assay

A-C. Representative images for Fig. 4B; COS7 cells transfected with GFP (**A**), mycNLS-α-cat 1-163 (**B**), or mycNLS-WT-α-cat (**C**) were incubated in cell culture media supplemented with 2 mM BrU for one hour. Immunofluorescence images for myc, BrU, Hoechst, and merged images are shown. Arrows indicate transfected cells in panel C. Scale bar =20 μm.

Fig. S13: Immunofluroescene images for BrU quantification

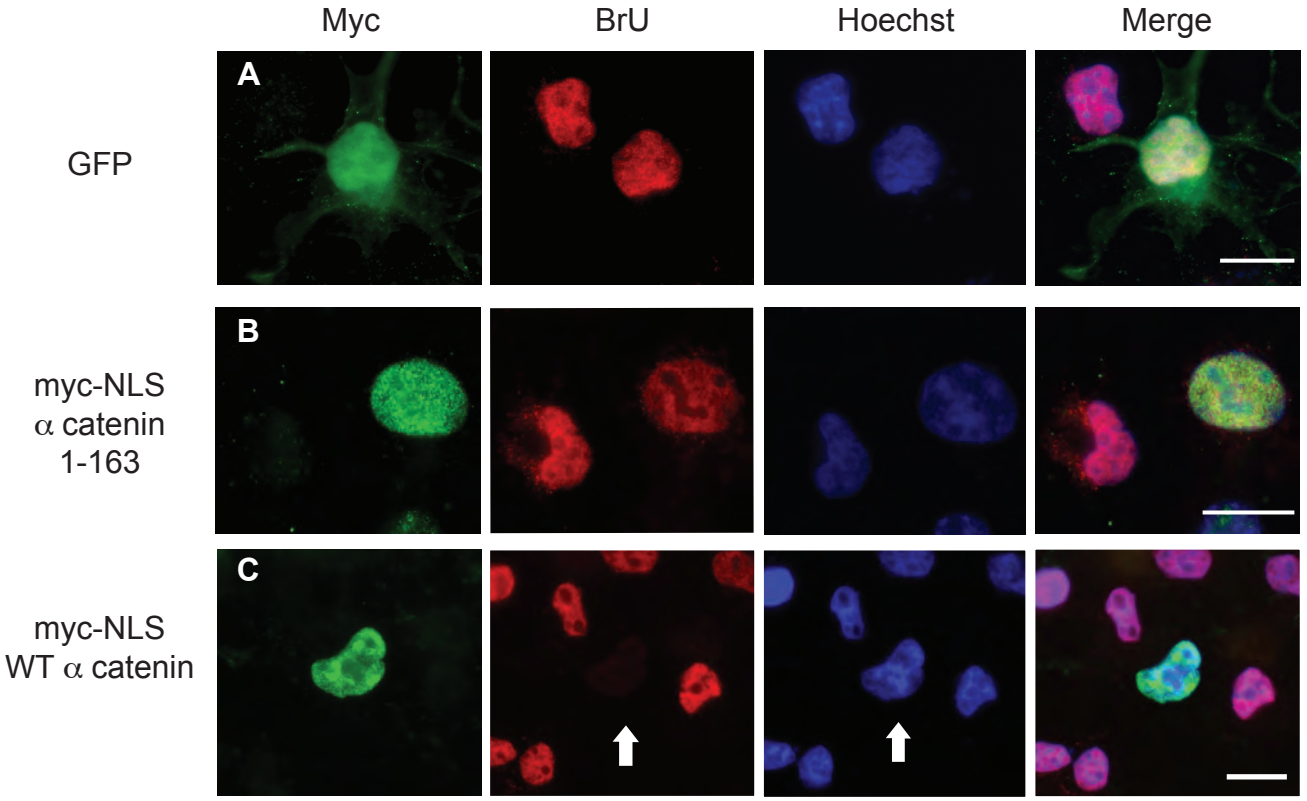

Figure S14: α-Cat silencing leads to enhanced transcription in an *in vitro* assay

Upper gel: Autoradiograph of ^{32}[P]-labeled RNA transcripts from an adenovirus major late promoter (AdMLP) cassette incubated with nuclear extracts from control (non-specific hairpin, NS) and α-cat silenced SW480 cells using two independent α-cat hairpins. α-E-cad shRNA.1 corresponds to that used in Fig. 5; α-E-cad shRNA.2 targets the 3'UTR of α-cat (Sigma, Cat#: TRCN0000062653; Sense: CCACATTAGCTTGTTAGTAA). **Middle and lower gels:** Immunoblot of SW480 nuclear extracts from transcription assay (upper gel). Note that α-cat is effectively silenced relative to total nuclear actin and RNA Pol II, which are unchanged. Brackets refer to immunoblots from the same gel.

Fig. S14: Knock-down of α-cat in SW480 cells enhances transcription in an in vitro assay

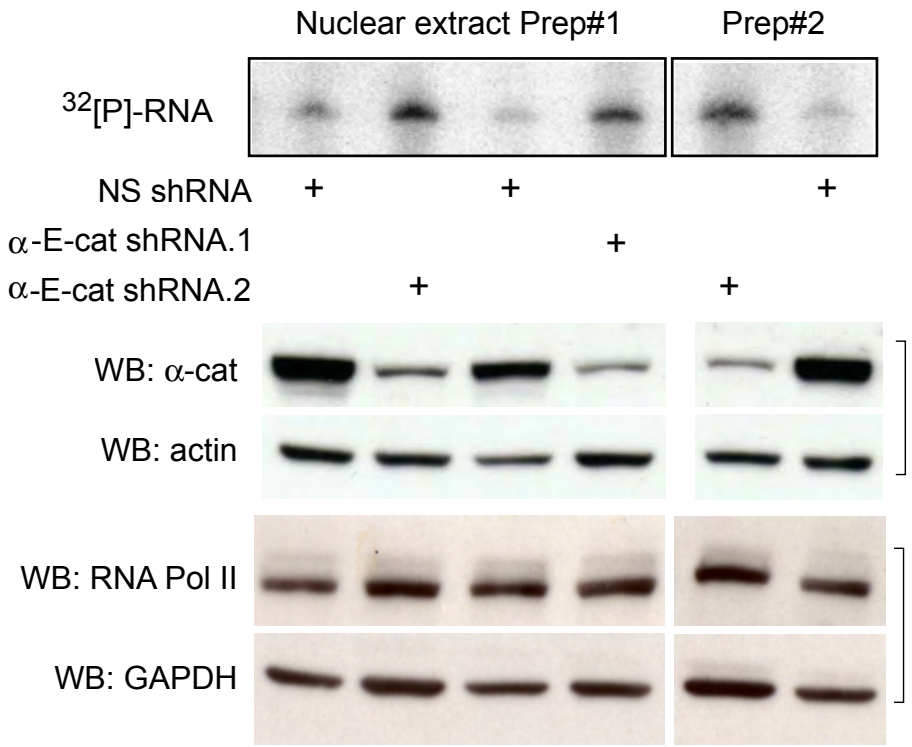

Figure S15: β-cat attenuates general transcription by EU incorporation in Cos7 cells

Representative immunofluorescence double-labeling image of Cos 7 cells transiently transfected with a myc-full-length β-cat expression vector (FL-β-catenin). Thirty hours post-transfection, cells were pulse-labeled for 15 minutes with 5-ethnyl uridine (EU, an alkyne-modified nucleotide that becomes actively incorporated into nascent RNAs), fixed and stained for β-cat (red), RNA (green) and DNA (Hoechst blue). Scale bar =20 μm. Note that β-cat positive cells on average manifest reduced EU incorporation compared with adjacent untransfected cells (Quantified in Fig. 6D).

Fig. S15: β-cat attenuates general transcription (EU incorporation) in Cos7 cells

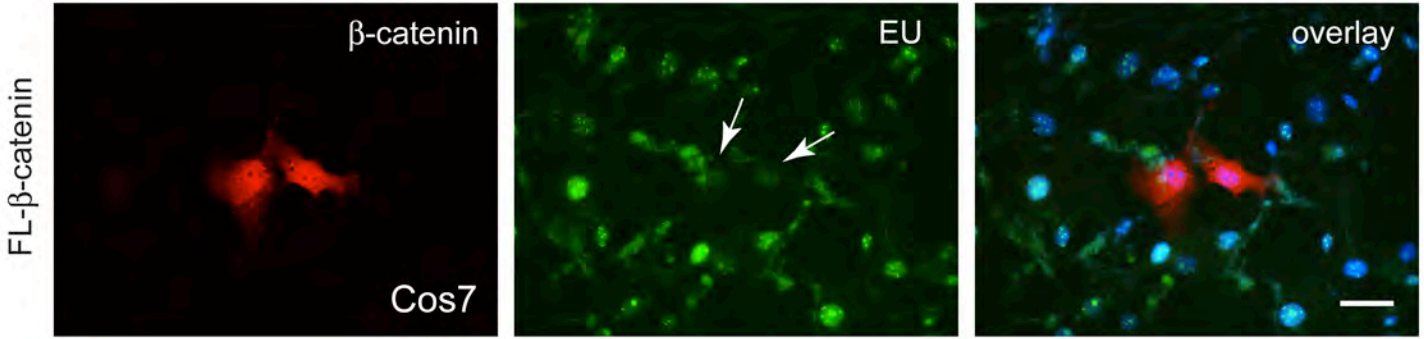

Figure S16: Model

We show that β-cat/TCF loading on promoters (e.g., *TOP, LEF1* and *C-MYC*) is not impacted by the absence (A) or presence (B) of α-cat, indicating that α-cat-mediated inhibition of these genes is down-stream of β-cat/TCF loading. Previous studies show that actin monomers (red circles) incorporate into all three RNA polymerases (e.g., Pol I-III) as well as chromatin remodeling complexes, and thus is required for transcription. Evidence that α-cat silencing leads to an increase in actin recruitment to the *C-MYC* promoter is consistent with a model where α-cat attenuates transcription through impacting nuclear actin dynamics. Nuclear targeted and over-expressed α-cat promotes formation of nuclear F-actin filaments and reduces RNA synthesis, possibly through diverting nuclear actin monomers into polymers. The ability of α-cat to limit both β-cat/TCF-specific and general transcription may be explained by existence of distinct nuclear pools of α-cat (i-iii), where promoter-localized α-cat (i) inhibits Wnt-specific genes, but the diffuse nucleoplasmic pool of α-cat (ii-iii) may impact transcription more generally via nuclear actin.

Fig. S16: Model

A.

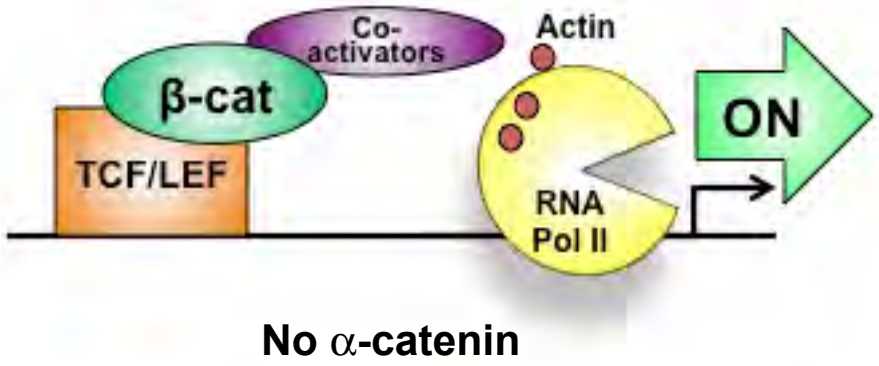

No α-catenin

B.

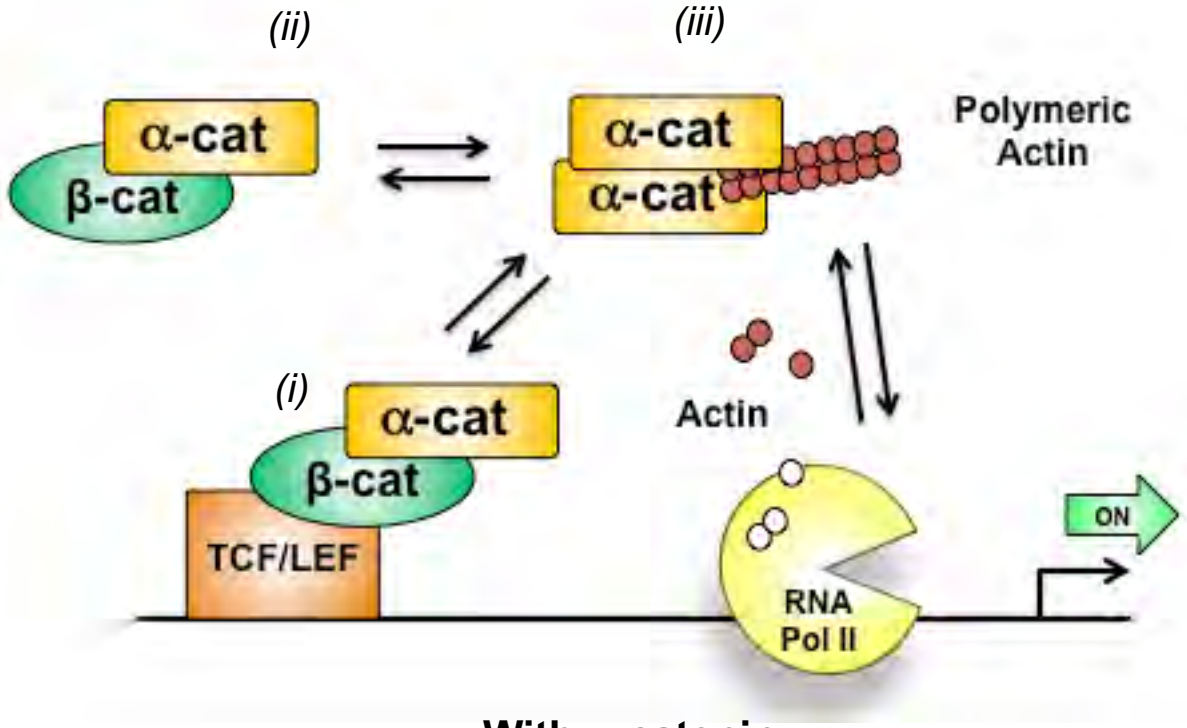

(i) Wnt/β-cat target gene effects?

(ii-iii) General transcription effects?

With α-catenin

Supplemental Movie Z-Stack 1:

Z-stacks of images were obtained in 1μm sections using a Zeiss LSM 710 confocal microscope with a 63x/1.46 oil alpha Plan Apochromat objective. Cos7 were transfected with the Myc NLS α-cat construct for 48 hours and prepared as described above. Cells were stained with rhodamine phalloidin (Invitrogen) to label actin filaments (red), FITC anti-myc antibody (Sigma) to label α-cat (green), and mounting media containing DAPI (Vectashield) to label DNA (blue). Image processing was done using Zeiss Zen software.

Supplemental Table 1

Quantitative Real time PCR primer sequences	
LEF-1	F: CAGAGAACACCCCGATGACGG
	R: CTGGAGAAAAGTGCTCGTCACTG
C-MYC	F: 5'-TGCGACGAGGAGGAGAACTT-3'
	R: 5'-TGGGCAGCAGCTCGAATTTC-3'
AXIN2	F: CCAACACCAGGCGGAACGAAG
	R: CGCCCAATAAGGAGTGTAAGGAC
MET	F: GCAATGGGGAGTGTAAAGAGG
	R: GCCCAGTCTTGTACTCAGCAAC
EDN-1	F: CACGTTGTTCCGTATGGACTTGG
	R: CACGGTCTGTTGCCTTTGTGG
DKK1	F: CCTTGAACTCGGTTCTCAATTCC
	R: CAATGGTCTGGTACTTATTCCCG
NKD1	F: GGGAAACTTCACTCCAAGCCG
	R: GTCTCCCGATCCACTCCTCG
NKX2.1	F: GCACACGACTCCGTTCTCAG
	R: GCCCACTTTCTTGTAGCTTTCC
NEDD9	F: GACCGTCATAGAGCAGAACACAG
	R: CTGCATGGGACCAATCAGAAGC
MMP7	F: GATGTGGAGTGCCAGATGTTGC
	R: CAGCAGTTCCCCATACAACTTTCC
CMYBP	F: GAGCTGCTTCGCCTAGAACTGG
	R: GAGGTGGTTCATACTGAGCAAGC
ANKRD1	F: GCCTACGTTTCTGAAGGCTGC
	R: GGCTGTGGATTCAAGCATATCACG
CTGF	F: GCAGCATGGACGTTCGTCTG
	R: CCACGGTTTGGTCCTTGGGC
GAPDH	F: CCTGGGCTACACTGAGCACC
	R: GTGGTCGTTGAGGGCAATGC
18SRNA	F: CTTAGAGGGACAAGTGGCGTTC
	R: CGCTGAGCCAGTCAGTGTAG
Primers for Chromatin IP qPCR	
4xTCF/LEF probe	Forward CAGTGCAGGGGAAAGAATAGTAGAC
	Reverse: TCTGCTTATATAGGCCTCCCACC
CMYC promoter	Forward: GGCACGGAAGTAATACTCCTCTCCTC
	Reverse: CTCCCCGGACAAACCGGACG
LEF-1 promoter:	Forward: GGCTGAGAAACTCGAGCCGGG
	Reverse: GGGCCGAGGAGGAGGGGAAG
Reference control with no TCF/LEF binding site	Forward: CCCAACTCCCACTGGCTTCAAG
	Reverse: GCCCAGCTTTCCTCTGGGCTG

Materials and Methods

Cell culture and antibodies

HEK293T, SW480 colon carcinoma, and COS7 cells were obtained from American Type Culture Collection and cultured in Dulbecco's Modified Eagle's Medium (DMEM) supplemented with penicillin/streptomycin (100U/ml) and 10% fetal bovine serum (FBS). Normal human fibroblasts (NHF) were isolated from newborn foreskins by the Skin Diseases Research Core at Northwestern University (Chicago, IL), and maintained in fibroblast growth media (LONZA, Cat#CC-3131). Only NHF propagated for no more than 8 passages were used for the experiments. Cells were incubated at 37°C and 5% CO_2. Antibodies used include mouse monoclonals to myc 9E10, beta tubulin (TUB2.1), and flag M2 (Sigma-Aldrich); α-cat (clone 5) and β-cat (clone 14, BD Transduction); α-cat mouse monoclonals 5B11, 3C1, 3H4 and 6A1 (2), acetylated histone H3 (Lys14) and BrdU/BrU (BU-1, Millipore), lamin A/C (5G4, Steve Adam, Northwestern University), anti-polymerase II (8WG16) and rabbit polyclonals to GFP and glyceraldehyde 3-phosphate dehydrogenase (GAPDH, Santa Cruz Biotechnology); Rhodamine-phalloidin and Alexa Fluor 488- and 568-conjugated goat IgGs (Invitrogen). Recombinant Wnt3a was purchased from R&D Systems. The primary Abs binding was detected with HRP-conjugated secondary Abs using ECL reagents (Pierce) or, when required, with secondary Abs conjugated with IR dyes (IRE-680 or IRE-800) using Odyssey IR scanner (LICOR, Lincoln, NB). Beta-Actin, GAPDH, LAMIN or HDAC1 were used as loading controls for cytoplasmic and nuclear proteins, respectively. Image digitizing and quantitative analysis were performed using the NIH-J and LI-COR software.

Plasmids and α-Cat knockdown

α-E-cat encoding regions were PCR amplified using PfuUltra High-Fidelity DNA polymerase (Stratagene) and subcloned into the EcoR1 and Not1 sites of pcDNA3. EYFP-NLS-actins (4) were previously described. Deletion of aa118-148 of β-cat was accomplished using the Quick Change method (Stratagene). Provided plasmids include: human Wnt3a pcDNA3 (H. Varmus, Sloan-Kettering, New York); luciferase-reporter plasmids 4x TOPflash, 4x FOPflash, and pol III-renilla (H. Clevers, Hubrecht Institute, Netherlands); WT-β-cat-flag (E. Fearon, University of Michigan); pGEX containing full-length human α-cat and N-terminal α-cat (aa 1-576) (D. Rimm, Yale University). To stably knock-down CTNNA1 the VSVG pseudotyped lentivirus expressing CTNNA1 hRNA was generated as described (5) (DNA/RNA Delivery Core, SDRC, Chicago IL) using 293T packaging cells (Gene Hunter Corporation, Nashville, TN), 2nd generation packaging vectors psPAX2 and pMD2.G (Addgene, Cambridge, MA) and 2nd generation lentiviral expression vector pGIPZ (Thermo Fisher Open Biosystems, Waltham, MA). The pGIPZ vector used encoded shRNA against CTNNA1 (shRNA α-cat.1: Cat# V2LHS_262377; sense: CCTGTTCCATCTCAAATAA; shRNA α-cat.2 (Sigma, Cat#: TRCN0000062653; Sense: CCACATTAGCTTGTTAGTAA), and non-silencing control shRNA (Cat# RHS4346; sense: TCTCGCTTGGGCGAGAGTAAG) (provided by the RNAi/Throughput Core, Northwestern University, Evanston, IL). Since lentiviral infection efficacy was > 90%, bulk cell populations, but not individual stably infected cell clones, were used to establish the following stable cell lines: SW480-shCTNNA1, SW480-Non-Silencing (NS), and primary normal human fibroblasts NHF-shCTNNA1 and NHF-NS. Stable cell lines were maintained in the presence of 8μg/ml puromycin. To

knock-down CTNNA1 for a short-term of 2-4 days, a pool of four siRNAs (Dharmacon, SMARTpool siGENOME library, Cat# M-010505-01, Waltham, MA) was transiently transfected into SW480 cells using Effectene transfection reagent (Qiagen, Valencia, CA) according to the manufactures recommendations at final concentration of 25 nM each (100 nM total of pooled siRNA) and experiments were performed 72 hr post-transfection.

Quantitative real-time PCR

All real-time quantitative PCR (qPCR) experiments were performed as described previously (6) using the iCycler MyiQ single color real-time PCR detection system (Bio-Rad Laboratories). Total RNA was isolated using the Aurum Total RNA mini kit (Bio-Rad) and cDNAs were synthesized using 1μg RNA with the iScript cDNA Synthesis kit (Bio-Rad). Endogenous gene expression was analyzed using primers (see Table 1) for the following human genes: MET, EDN1, DKK1, NKD1, CMYC, AXIN2, NKX2, MYCBP, MMP7, NEDD9, ANKRD1, and LEF-1. Expression of the targets genes was normalized to several reference proteins including GAPDH, L19, and human 18S. To decrease constitutive β-cat signaling, SW480 and NHF cells were starved in the serum free media for 24 hours and treated with recombinant 50-100 ng/ml Wnt3A when required. The Q-PCR was performed in triplicate and the data were analyzed with the ΔΔCt method using GAPDH/L19 or 18S Q-PCR signal as a reference gene.

Chromatin Immunoprecipitation

ChIP was performed as described in references (7-12) with commercial reagents (ChIP Kit Cat#17-295, Millipore). In brief, 30-50 x 10^6 SW480 cells at 70-80% confluence were starved in FBS free medium for 24 hrs and induced with 10% FBS for 2 hrs. Cells

were fixed with 1% formaldehyde at 37°C for 10 min to cross-link protein-DNA complexes following addition of 0.125 M Glycine for formaldehyde quenching. Cell were lysed (1% SDS, 10 mM EDTA, 50 mM Tris, pH 8.1), sonicated to generate 200–600 bp DNA fragments and diluted x10 with the antibody binding buffer (0.01% SDS, 1.1% Triton X-100, 1.2 mM EDTA, 16.7 mM Tris pH 8.1, 167 mM NaCl). The ChIP grade and concentrated Abs (all in amount of 10 μg) were used (gentle rocking, 4ºC for 12 hrs) to IP DNA complexes with the following proteins: α-cat clone 5B11 generated by the NU Recombinant Protein Core), β-cat (Cat# 7199X, Santa Cruz, San Diego, CA), TCF4 (official gene symbol TCF7L2) (Cat# CS204338, Millipore), beta-actin (clone AC-15 Cat# A5441, Sigma). A mixture of ChIP grade mouse and rabbit IgG (Millipore) were used as negative control. The antibody-bound protein-DNA complexes were captured with 100 μl mixture of 50 μl protein A and 50 μl G-agarose supplemented with salmon sperm DNA (Cat# 16-157C, Cat# 16-201 all from Millipore). The protein-A/G captured protein-DNA complexes were washed (gentle rocking for 5 minutes, 4ºC, centrifugation at 1000 rpm) with the x10 volumes of the following buffers: 3 times with low salt buffer (0.1% SDS, 1% Triton X-100, 2 mM EDTA, 20 mM Tris, 150 mM NaCl, pH 8.1), once with high salt buffer (0.1% SDS, 1% Triton X-100, 2 mM EDTA, 20 mM Tris, 500 mM NaCl, pH 8.1), once with immune complex wash buffer (0.25 M LiCl, 1% IGEPAL, 1% deoxycolic acid sodium salt, 1 mM EDTA, 10 mM TRIs, pH 8.1) and 2 times with TE buffer. The protein-DNA complexes were eluted (0.1 M $NaHCO_3$, 1% SDS at 65ºC) and cross-linking reversed (0.2 M NaCl, 65ºC for 8 hrs), with subsequent addition of RNAse A (1 ml, 37ºC for 30 min, Invitrogen Life Sciences) and proteinase K (25 mM EDTA, 0.1 M Tris, pH 6.5, 42ºC for 4 hrs). The resultant DNA fragments were purified on DNA

binding columns (Mini-elute kit, Cat# 28604, Qiagen). To study promoter-context independent regulation, we stably introduced a tandem of four canonical TCF/LEF sites (4xTCF/LEF probe, 5) into SW480 cells (SW480-shCTNNA1 and SW480-NS) using lentivirus. The primer sets yielding 150-200 bp product were designed to assess promoter loading of CMYC (10) and LEF-1 (11, 12) genes and 4xTCF4/LEF probe (7, 13). The positions of the TCF/LEF binding sites taken from the references (7, 10, 13, 14) were verified by the on-line search engine Transfac PATCH public 1.0 (Pattern Search for Transcription Factor Binding Sites, www.gene-regulation.com). As an additional reference control we analyzed loading to a sequence on the chromosome 8 (Chr 8: 128762215-128762493) containing no TCF/LEF binding sites as determined by the Transfac PATCH public 1.0. Sets of 1% aliquots of the cell lysates were taken as DNA and protein inputs. Quantitative analysis of the ChIPed DNA fragments was performed by SYBR Green Q-PCR (Cat#170-8880, Biorad). The Q-PCR data were analyzed by the fold enrichment method using ΔΔCt formula as described (7, 8). The experiments were performed three times on independently plated cells. To reduce the variability of the ChIP data, the DNA samples from the three experiments were Q-PCR analyzed at once within one 384 well-plate using all primer sets.

Fractionation of the extracellular compartments

SW480 cells (10-15^6 cells) were lysed with extraction buffer (50mM Tris-HCl, pH 7.4, 100 mM NaCl, 0.01% digitonin) with vigorous shaking for 30 min at 4ºC, and centrifuged at 10,000 rpm (5 min, 4ºC) to obtain clear cytoplasmic extract. The residual pellet was washed one additional time with the cytoplasmic extraction buffer and the

exchange buffer (25 mM Tris-HCl pH 7.4, 1 mM $MgCl_2$, 5 mM KCl, 1 mM DTT, 1% NP-40) each time with vigorous shaking for 10 minutes at 4ºC and centrifugation at 6000 rpm for 5 min at 4ºC. Membrane-associated proteins were solubilized in membrane extraction buffer with vigorous shaking for 30 min at 4ºC (50 mM Tris-HCl pH 7.4, 100 mM NaCl, 10% Triton) and clarified by centrifugation at 3,000 rpm (5 min, 4ºC). The resultant pellet (crude nuclear fraction) was washed two additional times with membrane extraction buffer and twice with the exchange buffer, each time with vigorous shaking for 10 minutes at 4ºC and centrifugation at 3,000 rpm for 5 min at 4ºC. To improve purity, the nuclear pellet was washed three times in 0.3 M Sucrose buffer (25 mM Tris-HCl pH 7.4, 1 mM $MgCl_2$, 5mM Kcl, 1 mM DTT, 1% NP-40, 0.3 M Sucrose) and three times in the 0.9 M Sucrose buffer (25 mM Tris-HCl pH 7.4, 1 mM $MgCl_2$, 5mM Kcl, 1 mM DTT, 1% NP-40, 0.9 M Sucrose), each time with vigorous shaking for 5 minutes at 4ºC and centrifugation at 3,000 rpm for 5 min at 4ºC. Sucrose was removed by two washes with exchange buffer with centrifugation at 3,000 rpm for 5 min at 4ºC. Nuclear proteins were solubilized in the nuclear extraction buffer (20 mM Tris-HCl pH 7.4, 400 mM NaCl, 1.5 mM $MgCl_2$,1% NP-40) and 2 U Benzonase (Sigma) to disintegrate DNA-protein complexes with vigorous shaking for 30 minutes at 4ºC and centrifugation at 14,000 rpm for 5 min at 4ºC to obtain clear nuclear extract. Cytoplasmic, membrane and nuclear extracts (80 μg per well) were analyzed by 4-20% gradient denaturing PAGE and immunoblots were analyzed using a LI-COR imaging system (Odyssey).

Protein interaction analysis

Protein interactions between α-cat, β-cat and TCF4/TCF7L2 were confirmed by Protein-Agarose (Cat# 20333, Millipore) and Ni-NTA agarose (Cat# 1018244, Millipore) pull-

down methods. For protein-A pull-down, SW480 cells were lysed, diluted x10 with the antibody-binding buffer and incubated with Abs to α-cat, β-cat and TCF4/TCF7L2 as described in the ChIP section. The Abs-bound protein-complexes were pulled down with Protein-A agarose, washed, eluted as described in the ChIP section and analyzed by Western Blotting. To verify interaction between α-cat and TCF4/TCF7L2, we introduced human α-cat fused at N terminus with a tandem tag consisting of 6xHis and TEV protease cleavage site (ENLYFQ) into R2/7 cells (R2/7-6xHis-TEV- α-cat cells) using lentivirus as described (15, 16). The R2/7-6xHis-TEV-α-cat cells were lysed as in ChIP section and incubated with Ni-NTA agarose (gentle rocking, 4ºC for 12 hrs). The α-cat-protein complexes captured by Ni-NTA agarose were washed as described in ChIP, clarified with 20mM imidazole washing buffer and eluted with addition of the TEV-protease (TEV added as 1:10 protein ratio with gentle rocking, 4ºC overnight; TEV buffer: 10 mM Tris-HCl pH 8.0, 150 mM NaCl, 0.1% IGEPAL CA-630, 1 mM DTT). The TEV-protease eluate was analyzed by Western blotting. The TEV-protease was provided by the Northwestern University Recombinant Protein Production Core Facility.

Wnt/β-cat signaling reporter Assay

Approximately $1.5x10^5$ HEK or SW480 cells were transfected with 4x TOPflash or 4x FOPflash, pol III-renilla, and α-cat using the Lipofectamine 2000 protocol. Wnt3a or β-cat co-transfection allowed for activation of the canonical Wnt pathway. All DNA concentrations were normalized with GFP. Cells were allowed to incubate 48 hours and were subsequently analyzed using the Dual-Luciferase Reporter Assay System (Promega)

and the Veritas Microplate Luminometer (Turner Biosystems). All experiments were performed in duplicate in 24-well format.

Immunofluorescence

Cells were plated on coverslips and allowed to spread for 48 hours. For fixation, cells were incubated in 4% formaldehyde and quenched with 10mM glycine. Subsequently, cells were permeabilized and blocked in a solution containing 0.3% Triton-X 100 and 1% bovine serum albumin in PBS. Primary antibodies were added to permeabilization buffer supplemented with 5% normal goat serum and allowed to incubate in a humid chamber for one hour. Fluorophore-conjugated secondary antibodies were added to NGS-supplemented buffer and incubated for an additional hour. Nuclei were stained with Hoechst 33342 (Invitrogen). F-actin was stained with Alexa-Fluor 594 conjugated phalloidin (Invitrogen). Coverslips were mounted in ProLong Gold Antifade Reagent (Invitrogen). All slides were imaged on the Zeiss Axiovision 2 fluorescent microscope equipped with a 63x Plan-Neofluar NA 1.25 objective and AxioVision4.6 software (Carl Zeiss, Inc.). All immunofluorescent images were further processed with Photoshop CS3 (Adobe).

EU Labeling Experiments

COS-7 cells were transfected in suspension with 1μg full-length β-cat (FL β-cat) or β-cat having a deletion in the α-cat binding domain (β-cat-Δα-catBD) at 1μg DNA/150,000 cells using Lipofectamine 2000 reagent (Life Technologies Corp.) according to manufacturer instructions. Cells were plated to coverslips in Opti-MEM media (Life

Technologies Corp.). Media was changed after 24h to DMEM-10%FBS (Corning-Mediatech and Atlanta Biologicals). 48h after transfection, cells were treated with 1mM 5-ethynyl uridine (EU) (Life Technologies Corp.) in serum-free DMEM for 15 min at 37^0C. No-EU control cells were treated with PBS alone. Cells were fixed in 3% paraformaldehyde in PBS for 15 min, then permeabilized with 3% BSA in PBS-0.3% TX-100 for 15 min. EU uptake was detected with the Click-It Cell Reaction Buffer Kit (Life Technologies Corp.) and Alexa Fluor 488-azide (Life Technologies Corp.), applied for 30 min according to manufacturer directions. Cells were then co-stained using standard immunofluorescence methods with rabbit anti-β-catenin (EMD Millipore) and Alexa Fluor 568 goat anti-rabbit IgG (Life Technologies Corp.). Nuclei were stained using Hoechst 33342 (Life Technologies Corp.). Coverslips were mounted to slides with AquapolyMount (Polysciences, Inc), and imaged at fixed exposure with 63x objective on a Zeiss Axioplan 2 microscope. Average fluorescence intensity of EU in cell nuclei from 40 images per condition was quantified using MetaMorph software (Molecular Devices). Red cells were scored as positive for β-cat expression.

Transcription Assay and RNA Synthesis

In vitro transcription assays were performed using nuclear extracts from control and α-cat silenced SW480 cells. Nuclear extracts were prepared by the procedure of Dignam et al (17). The DNA template was a negatively supercoiled plasmid DNA containing the adenovirus major late promotor (AdMLP) fused to a 380bp G-less cassette (18). Nuclear extracts were pre-incubated with indicated amounts of recombinant α-cat for 30 minutes

on ice. Nucleotides and DNA templates were then added to initiate transcription. After incubating for 30 min at 30°C, the transcription products were extracted and separated by 6% polyacrylamide, 7M urea denaturing gel electrophoresis and visualized using a phosphorimager (Molecular Dynamics, Amersham). To quantify RNA synthesis in vivo, COS7 cells were transfected with indicated plasmids and allowed to incubate for 36-48 hours. On the day of the experiment, cell culture media was supplemented with 2mM bromouridine (BrU; Sigma) or 1mM 5-ethynyl uridine (EU) (Life Technologies Corp.) in serum-free DMEM for 15 min at 37^0C (or time indicated). Cells were then fixed in 3% paraformaldehyde and labeled for α-cat (or β-cat) and BrU (or EU) as described in the Supplement. Average fluorescence intensity of EU in cell nuclei from transfected versus adjacent untransfected cells was quantified using MetaMorph software (Molecular Devices).

Nuclear actin sedimentation assay

Nuclear extracts were isolated as described above. Equal concentrations of nuclear extracts were spun at 100,000g for 1hr at 4°C. The supernatant and pellet fractions were separated, boiled in hot SDS loading buffer, and briefly sonicated. Samples were then run on SDS-PAGE and western blotted for Actin (C4 antibody, Millipore). Band intensity was quantified using ImageJ. Actin band intensity in the pellet fractions was normalized to band intensity in the pellet plus supernatant.

Nuclear Actin Filament Expression

SW480 NS shRNA and SW480 α-E-catenin shRNA stable cell lines were transiently transfected with NLS β-actin EYFP (4) or V163M α-actin EGFP (3) for 48hrs to induce nuclear actin filaments. Cells were fixed in 4% PFA and imaged. The number of nuclei with nuclear actin filaments was counted as a function of the total number of transfected cells.

FRAP Microscopy and Analysis

FRAP was performed using a Zeiss LSM 710 confocal microscope with a 63x/1.46 Oil alpha Plan-Apochromat objective. SW480 NS shRNA and SW480 α-E-catenin shRNA stable cell lines were transiently transfected with NLS β-actin EYFP (4) for 48hrs. Only cells that did *not* have nuclear actin filaments due to NLS β-actin EYFP expression were analyzed by FRAP. To perform FRAP, 5 pre-bleach images were taken then nuclei were bleached in ~1μm circles at 100% 488nm laser power for 25 iterations. Images were collected at 0.5msecs for a total of 50 secs. Fluorescence intensity was normalized to pre-bleach intensity, and corrected for non-specific photobleaching and background using the Zeiss FRAP module. Images were acquired from two separate experiments. A biphasic recovery curve was fit to the data based on goodness of fit (R^2=.97; N=21 and R^2=.94; N=19 for SW480 NS shRNA and Sw480 α-E-cat shRNA respectively) and previous studies (19). Graphing analysis and curve fitting was performed using Graphpad Prism.

Statistics

Statistical significance was determined by the unpaired Student's t test. P value is indicated by asterisk or asterisks in the figures: * denotes $P<0.05$; **, $P<0.01$; ***, $P<0.001$.

References

1. Benjamin JM, *et al*. (2010) AlphaE-catenin regulates actin dynamics independently of cadherin-mediated cell-cell adhesion. *The Journal of cell biology* 189(2):339-352.
2. Roe S, Koslov ER, & Rimm DL (1998) A mutation in alpha-catenin disrupts adhesion in clone A cells without perturbing its actin and beta-catenin binding activity. *Cell adhesion and communication* 5(4):283-296.
3. Domazetovska A, *et al*. (2007) Mechanisms underlying intranuclear rod formation. *Brain* 130(Pt 12):3275-3284.
4. Hofmann WA, *et al*. (2009) SUMOylation of nuclear actin. *The Journal of cell biology* 186(2):193-200.
5. Naldini L, *et al*. (1996) In vivo gene delivery and stable transduction of nondividing cells by a lentiviral vector. *Science* 272(5259):263-267.
6. Maher MT, Flozak AS, Stocker AM, Chenn A, & Gottardi CJ (2009) Activity of the beta-catenin phosphodestruction complex at cell-cell contacts is enhanced by cadherin-based adhesion. *The Journal of cell biology* 186(2):219-228.
7. Mukhopadhyay A, Deplancke B, Walhout AJ, & Tissenbaum HA (2008) Chromatin immunoprecipitation (ChIP) coupled to detection by quantitative real-time PCR to study transcription factor binding to DNA in Caenorhabditis elegans. *Nature protocols* 3(4):698-709.
8. Sikes ML, *et al*. (2009) A streamlined method for rapid and sensitive chromatin immunoprecipitation. *Journal of immunological methods* 344(1):58-63.
9. Yemelyanov A, *et al*. (2012) Differential targeting of androgen and glucocorticoid receptors induces ER stress and apoptosis in prostate cancer cells: a novel therapeutic modality. *Cell cycle* 11(2):395-406.
10. Sierra J, Yoshida T, Joazeiro CA, & Jones KA (2006) The APC tumor suppressor counteracts beta-catenin activation and H3K4 methylation at Wnt target genes. *Genes & development* 20(5):586-600.
11. Liu X, *et al*. (2010) Sox17 modulates Wnt3A/beta-catenin-mediated transcriptional activation of the Lef-1 promoter. *American journal of physiology. Lung cellular and molecular physiology* 299(5):L694-710.
12. Filali M, Cheng N, Abbott D, Leontiev V, & Engelhardt JF (2002) Wnt-3A/beta-catenin signaling induces transcription from the LEF-1 promoter. *The Journal of biological chemistry* 277(36):33398-33410.
13. Shih IM, Yu J, He TC, Vogelstein B, & Kinzler KW (2000) The beta-catenin binding domain of adenomatous polyposis coli is sufficient for tumor suppression. *Cancer research* 60(6):1671-1676.
14. He TC, *et al*. (1998) Identification of c-MYC as a target of the APC pathway. *Science* 281(5382):1509-1512.
15. Miladi B, *et al*. (2013) An Improved Strategy for Easy Process Monitoring and Advanced Purification of Recombinant Proteins. *Molecular biotechnology*.
16. Sun C, *et al*. (2012) Tobacco etch virus protease retains its activity in various buffers and in the presence of diverse additives. *Protein expression and purification* 82(1):226-231.

17. Dignam JD, Lebovitz RM, & Roeder RG (1983) Accurate transcription initiation by RNA polymerase II in a soluble extract from isolated mammalian nuclei. *Nucleic acids research* 11(5):1475-1489.
18. Kugel JF & Goodrich JA (2000) A kinetic model for the early steps of RNA synthesis by human RNA polymerase II. *The Journal of biological chemistry* 275(51):40483-40491.
19. McDonald D, Carrero G, Andrin C, de Vries G, & Hendzel MJ (2006) Nucleoplasmic beta-actin exists in a dynamic equilibrium between low-mobility polymeric species and rapidly diffusing populations. *The Journal of cell biology* 172(4):541-552.